Available online at www.sciencedirect.com
ScienceDirect
Journal of the European Ceramic Society 31 (2011) 265–272
www.elsevier.com/locate/jeurceramsoc

Microwave dielectric properties of $Ba_3Ti_{4-x}(Zn_{1/3}Nb_{2/3})_xNb_4O_{21}$ for low temperature co-fired ceramics

Qi-Long Zhang, Dong Zou, Hui Yang *

Department of Materials Science and Engineering, Zhejiang University, Hangzhou 310027, China

Received 6 May 2010; received in revised form 17 September 2010; accepted 27 September 2010
Available online 27 October 2010

Abstract

The effects of substitution of $(Zn_{1/3}Nb_{2/3})$ for Ti on the sintering behavior and microwave dielectric properties of $Ba_3Ti_{4-x}(Zn_{1/3}Nb_{2/3})_xNb_4O_{21}$ $(0 \le x \le 4)$ ceramics have been investigated. The dielectric constant (ε_r) and the temperature coefficient of the resonant frequency (τ_f) of $Ba_3Ti_{4-x}(Zn_{1/3}Nb_{2/3})_xNb_4O_{21}$ ceramics decreased with increasing x. However, the $Q \times f$ values enhanced with the substitution of $(Zn_{1/3}Nb_{2/3})$ for Ti. It was found that a small amount of $MnCO_3$–CuO (MC) and ZnO–B_2O_3–SiO_2 (ZBS) glass additives to $Ba_3Ti_{4-x}(Zn_{1/3}Nb_{2/3})_xNb_4O_{21}$ $(x = 2)$ ceramics lowered the sintering temperature from 1250 to 900 °C. And $Ba_3Ti_{4-x}(Zn_{1/3}Nb_{2/3})_xNb_4O_{21}$ $(x = 2)$ ceramics with 1 wt% MC and 1 wt% ZBS sintered at 900 °C for 2 h showed excellent dielectric properties: $\varepsilon_r = 53$, $Q \times f = 14{,}600$ GHz, $\tau_f = 6$ ppm/°C. Moreover, it has a chemical compatibility with silver, which made it as a promising material for low temperature co-fired ceramics technology application.

Keywords: LTCC; X-ray methods; Dielectric properties; Glass ceramics; Substrates

1. Introduction

Low temperature co-fired ceramics (LTCC) for microwave applications has received much attention because of their potential application for novel multi-layer communication modules involving the integration of passive components. The major requirements for these materials are low sintering temperature which should be below the electrode metals (Ag or Cu) melting temperature, excellent chemical compatibility with metals in the sintering process, as well as good microwave properties.[1] Several microwave dielectric ceramic systems, including MgO–TiO_2, BaO–TiO_2, (Zr, Sn)TiO_4, Li_2O–Nb_2O_5–TiO_2, CaO–Li_2O–Nb_2O_5–TiO_2 and BaO–Ln_2O_3–TiO_2 (Ln = La, Nd, Sm),[2–7] have been reported for applications using low-melting glass frits or oxides.

Recently, the microwave dielectric properties of several ceramics in the BaO–TiO_2–Nb_2O_5 system such as $BaTi_3Nb_4O_{17}$, $Ba_6Ti_{14}Nb_2O_{19}$, $Ba_3Ti_5Nb_6O_{28}$ and $Ba_3Ti_4Nb_4O_{21}$ have been reported.[8–10] Among these ceramics, $Ba_3Ti_4Nb_4O_{21}$ revealed a high permittivity of 55 and an excellent $Q \times f$ value of 9000 GHz. However, $Ba_3Ti_4Nb_4O_{21}$ ceramics also possessed a large positive τ_f value which precludes their usage in practice. Although several methods were investigated to tune τ_f to as closed as zero.[11,12] However, the τ_f value was still quite positive (50 ppm/°C) and the $Q \times f$ values decreased seriously. It has been reported that the substitution of $(Zn_{1/3}Nb_{2/3})$ for Ti in complex perovskite materials such as $Ba(Zn_{1/3}Nb_{2/3})O_3$ and $Ca(Zn_{1/3}Nb_{2/3})O_3$ can strongly influence microwave dielectric properties.[13,14] In order to develop a mid-permittivity LTCC material based on $Ba_3Ti_4Nb_4O_{21}$, the effects of the substitution of $(Zn_{1/3}Nb_{2/3})$ for Ti on the sintering behavior and microwave dielectric properties of $Ba_3Ti_{4-x}(Zn_{1/3}Nb_{2/3})_xNb_4O_{21}$ $(0 \le x \le 4)$ ceramics were firstly studied, and then the multiple additive consisted of $MnCO_3$–CuO and ZBS glass were chosen as a sintering aid to lower the sintering temperature of $Ba_3Ti_{4-x}(Zn_{1/3}Nb_{2/3})_xNb_4O_{21}$ $(x = 2)$ ceramics. Moreover, the chemical compatibility of silver electrodes and the LTCC materials have also been investigated.

2. Experimental procedure

$Ba_3Ti_{4-x}(Zn_{1/3}Nb_{2/3})_xNb_4O_{21}$ $(0 \le x \le 4)$ ceramics were prepared by the conventional solid-state reaction method.

* Corresponding author. Tel.: +86 571 87951408; fax: +86 571 87951408.
E-mail addresses: mse237@zju.edu.cn, yanghui@zju.edu.cn (H. Yang).

0955-2219/$ – see front matter © 2010 Elsevier Ltd. All rights reserved.
doi:10.1016/j.jeurceramsoc.2010.09.018

The stoichiometric mixtures of $BaCO_3$ (≥99%), Nb_2O_5 (≥ 99%), TiO_2 (≥ 98%) and ZnO (≥ 99%) powders were weighed and milled in ethanol medium for 24 h using zirconia balls. The wet powders were dried and calcined in air at 1100 °C for 4 h. For $MnCO_3$–CuO (MC), $MnCO_3$ (≥99%) and CuO (≥99%) were weighed according to the compositions of $0.2MnCO_3$–0.8CuO and calcined at 750 °C for 3 h. The $Ba_3Ti_{4-x}(Zn_{1/3}Nb_{2/3})_xNb_4O_{21}$ ($x = 2$) powders were remilled with MC and home-made ZnO–B_2O_3–SiO_2 (ZBS) additives for 24 h. The dried powders were mixed 5% PVA solution and subsequently uniaxially pressed into cylindrical pellets of 18 mm in diameter and 7–9 mm in thickness under a pressure of 80 MPa. The samples were sintered at different temperatures for 2 h with a heating and cooling rate of 5 °C/min.

The bulk densities of the ceramics were measured by the Archimedes method. The crystalline structures of the sintered samples were characterized by X-ray powder diffraction using Cu K_a radiation (XRD, Rigaku D/max-RA). For microstructural examination, the sintered ceramics were polished and thermally etched (100 °C below the sintering temperature) in air for 30 min. The microstructures of polished and thermally etched samples were observed by scanning electron microscopy (SEM, FEI SIRION-100) and the compositions were analyzed by energy-dispersive spectroscopy (EDS, EDAX GENENIS-4000). The dielectric constant (ε_r) and the quality factor values (Q) at microwave frequencies were measured using the Hakki–Coleman dielectric resonator method as modified and improved by Courtney,[15,16] using a network analyzer (Agilent 8719 Et, 0.05–13.5 GHz). The temperature coefficient of the resonant frequency (τ_f) was also measured by the same method by changing temperature from 25 °C to 80 °C and calculated from the equation:

$$\tau_f = \frac{f_{80} - f_{25}}{f_{25} \times 55} \times 10^6 (\text{ppm/°C}), \quad (1)$$

where f_{80} and f_{25} represented the resonant frequency at 80 °C and 25 °C, respectively.

3. Results and discussion

Fig. 1 shows the X-ray diffraction patterns of $Ba_3Ti_{4-x}(Zn_{1/3}Nb_{2/3})_xNb_4O_{21}$ ($0 \le x \le 4$) ceramics sintered at 1250 °C for 2 h. A single solid solution phase that corresponded to hexagonal $Ba_3Ti_4Nb_4O_{21}$ structure was obtained through the entire compositions. The diffraction peaks shifted to lower angles of 2θ gradually with increasing x content. The unit cell data and theoretical densities calculated from the diffraction data are presented in Table 1. It can be observed that the unit cell volume increased after substitutions, which was mainly attributed to the substitution of a larger ionic radius of $(Zn_{1/3}Nb_{2/3})^{4+}$ than that of Ti^{4+}.

Fig. 2 shows the relative densities of $Ba_3Ti_{4-x}(Zn_{1/3}Nb_{2/3})_xNb_4O_{21}$ ($0 \le x \le 4$) ceramics sintered at different temperatures. The relative density of $Ba_3Ti_4Nb_4O_{21}$ ceramics increased sharply with increasing temperature and had a constant value above 1280 °C. However, the relative densities of $Ba_3Ti_{4-x}(Zn_{1/3}Nb_{2/3})_xNb_4O_{21}$ ($0.5 \le x \le 2$) and

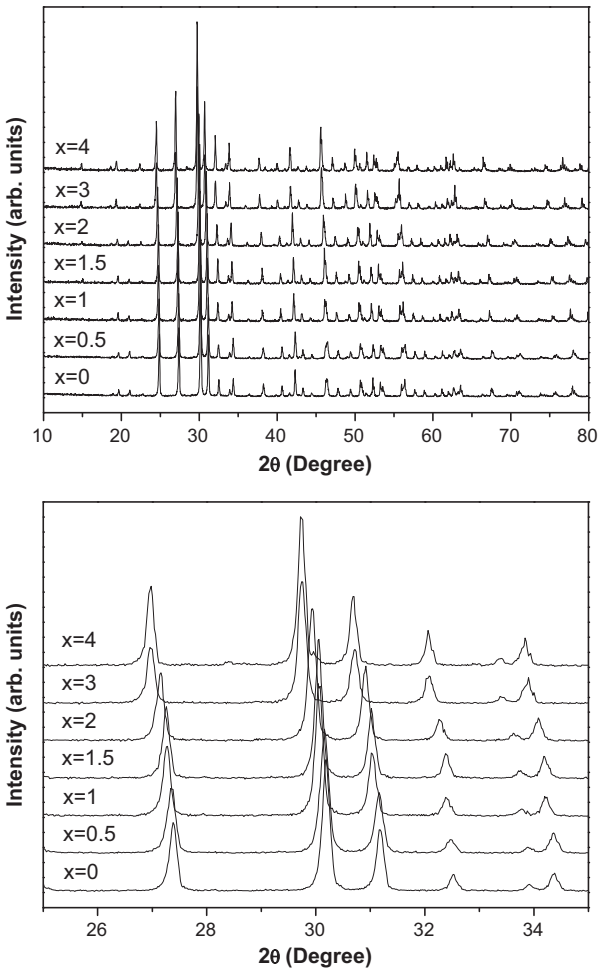

Fig. 1. X-ray diffraction patterns of $Ba_3Ti_{4-x}(Zn_{1/3}Nb_{2/3})_xNb_4O_{21}$ ($0 \le x \le 4$) ceramics sintered at 1250 °C for 2 h.

$Ba_3Ti_{4-x}(Zn_{1/3}Nb_{2/3})_xNb_4O_{21}$ ($3 \le x \le 4$) samples reached the maximum values at 1250 °C and 1220 °C, respectively. As shown in Fig. 1, $Ba_3Ti_{4-x}(Zn_{1/3}Nb_{2/3})_xNb_4O_{21}$ ($0.5 \le x \le 4$) could form solid solution by the substitution of $(Zn_{1/3}Nb_{2/3})$ for Ti. It indicates that the formation of solid solution could

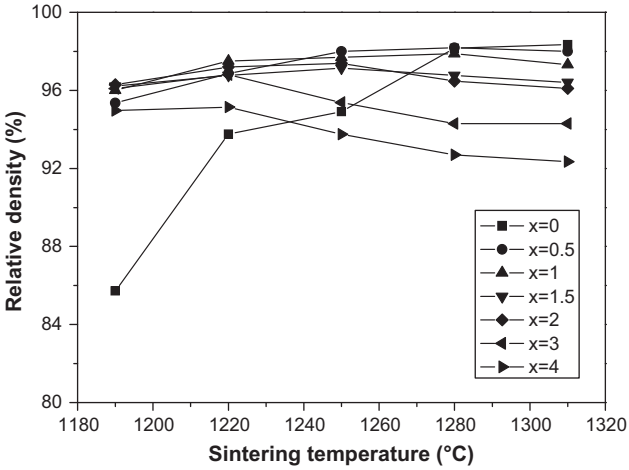

Fig. 2. Relative densities of $Ba_3Ti_{4-x}(Zn_{1/3}Nb_{2/3})_xNb_4O_{21}$ ($0 \le x \le 4$) ceramics sintered at different temperatures.

Table 1
The unit cell data and theoretical densities calculated from XRD patterns of $Ba_3Ti_{4-x}(Zn_{1/3}Nb_{2/3})_xNb_4O_{21}$ ceramics sintered at 1250 °C for 2 h.

x	a (Å)	c (Å)	Unit cell volume (Å^3)	Structure	Theoretical density (g cm^{-3})
0	9.0380	11.7771	833.13	Hexagonal, space	5.226
0.5	9.0410	11.7733	833.47	group: P63/mcm(193)	5.296
1	9.0196	11.9068	838.88		5.333
1.5	9.0639	11.8116	840.38		5.394
2	9.0434	11.8115	843.99		5.442
3	9.0766	11.8384	844.63		5.578
4	9.0456	11.9450	846.43		5.707

reduce the sintering temperature. However, the maximum relative density decreased from 98.3% to 95.1% with the x value increasing from 0 to 4. Moreover, the relative densities of $Ba_3Ti_{4-x}(Zn_{1/3}Nb_{2/3})_xNb_4O_{21}$ ($3 \le x \le 4$) decreased at higher temperatures, which was owing to that excessively high sintering temperature caused inhomogeneous grain growth (Fig. 3c and d) resulting in a decrease in density. SEM micrographs of the surfaces of $Ba_3Ti_{4-x}(Zn_{1/3}Nb_{2/3})_xNb_4O_{21}$ sintered at 1250 °C are illustrated in Fig. 3. The $Ba_3Ti_{4-x}(Zn_{1/3}Nb_{2/3})_xNb_4O_{21}$ sample with $x = 0.5$ had some pores and the grain size was small, approximately 1–2 μm. A dense structure could be obtained for $x = 1$. The increase of x leads to the promotion of the grain growth and a relative increase in the grain size can be achieved as illustrated in Fig. 3b–d. However, as the x is increased to ≥3, abnormal grain growth takes place leading to the presence of some large pores. As shown in Fig. 3c, the width of the largest grain was larger than 15 μm for $x = 3$. Abnormal grain growth can interfere with densification of ceramics.

Fig. 4 shows dielectric constant (ε_r) and quality factor values ($Q \times f$) values of $Ba_3Ti_{4-x}(Zn_{1/3}Nb_{2/3})_xNb_4O_{21}$ measured at 4–5 GHz. For each $Ba_3Ti_{4-x}(Zn_{1/3}Nb_{2/3})_xNb_4O_{21}$ composition, the variation of ε_r with sintering temperature is consistent with the trend of relative density. ε_r is also strongly dependent on $Ba_3Ti_{4-x}(Zn_{1/3}Nb_{2/3})_xNb_4O_{21}$ compositions. The maximum ε_r decreases from 66 for $x = 0$ to 45 for $x = 4$. In general, ε_r was dependent not only on the density and secondary phases, but also on the ionic polarizabilities. The relative densities of $Ba_3Ti_{4-x}(Zn_{1/3}Nb_{2/3})_xNb_4O_{21}$ ceramics corresponding to the maximum ε_r were higher than 95%. Hence, the ε_r was not significantly affected by the density, and there were no secondary phases through the entire composition range. Therefore, the ε_r was largely dependent on the ionic polarizability of the cations.[17] Shannon[18] reported the various ionic polarizabilities of the cations and the total molar dielectric polarizability of a compound can be calculated as a simple linear combination of individual ion dielectric polarizabilities. Therefore, $\alpha(Zn_{1/3}Nb_{2/3})^{4+}$ is straightforwardly expressed as:

$$\alpha(Zn_{1/3}Nb_{2/3})^{4+} = \frac{1}{3}\alpha(Zn^{2+}) + \frac{2}{3}\alpha(Nb^{5+}). \quad (2)$$

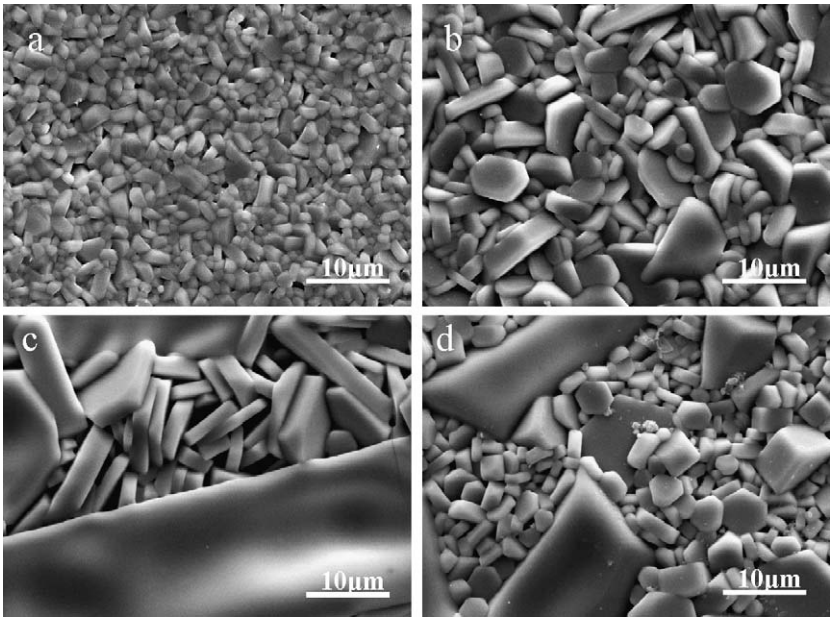

Fig. 3. SEM micrographs of $Ba_3Ti_{4-x}(Zn_{1/3}Nb_{2/3})_xNb_4O_{21}$ ceramics sintered at 1250 °C for 2 h: (a) $x = 0.5$, (b) $x = 1$, (c) $x = 3$, (d) $x = 4$.

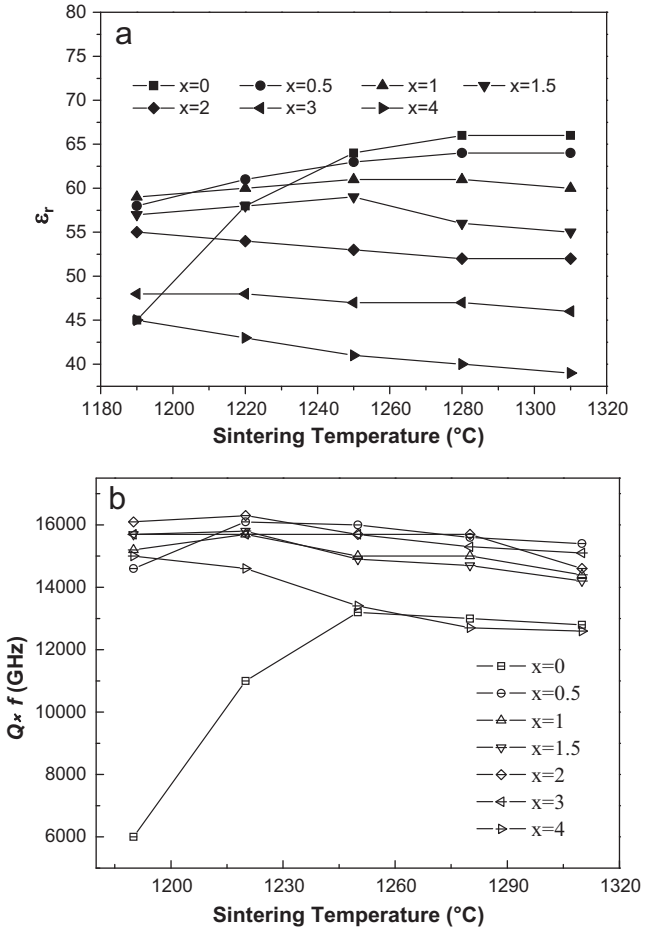

Fig. 4. Dielectric constants and the $Q \times f$ values of $Ba_3Ti_{4-x}(Zn_{1/3}Nb_{2/3})_xNb_4O_{21}$ $(0 \le x \le 4)$ ceramics as a function of sintering temperature.

Thus, the value of $\alpha(Zn_{1/3}Nb_{2/3})^{4+} = 3.33\ Å^3$ ($Zn^{2+} = 2.04\ Å^3$, $Nb^{5+} = 3.97\ Å^3$) is larger than Ti^{4+} ($2.93\ Å^3$). It is suggested that an increase in the dielectric constant takes place with the $(Zn_{1/3}Nb_{2/3})^{4+}$ substitution for Ti^{4+}. The dielectric constant of $Ba_3Ti_{4-x}(Zn_{1/3}Nb_{2/3})_xNb_4O_{21}$ in the composition range of 0–4, however, decreased as shown in Fig. 4. Therefore, the variation in the dielectric constant of $Ba_3Ti_{4-x}(Zn_{1/3}Nb_{2/3})_xNb_4O_{21}$ is considered to extremely depend on the crystal structure of ceramics. Ogawa et al.[19] suggested that the enhanced covalency of Sb–O bond in the octahedron by the Sb–O substitution for Nb–O lowers the dielectric constant. Thus, the dielectric constant of $Ba_3Ti_{4-x}(Zn_{1/3}Nb_{2/3})_xNb_4O_{21}$ decreased with increasing x, which may be due to that the covalency of Zn–O and Nb–O have more stronger covalency bond than that of Ti–O bonds in the AO_6 octahedra. It can be seen from Fig. 4b that the $Q \times f$ values enhanced after $(Zn_{1/3}Nb_{2/3})$ substituting for Ti except $Ba_3Ti_{4-x}(Zn_{1/3}Nb_{2/3})_xNb_4O_{21}$ with $x = 4$. Unfortunately, the reason is not unclear.

Fig. 5 shows the τ_f of $Ba_3Ti_{4-x}(Zn_{1/3}Nb_{2/3})_xNb_4O_{21}$ $(0 \le x \le 4)$ ceramics sintered at 1250 °C. The value of τ_f rapidly decreased with increasing x. The temperature coefficient of the resonant frequency (τ_f) is related to the temperature coefficient

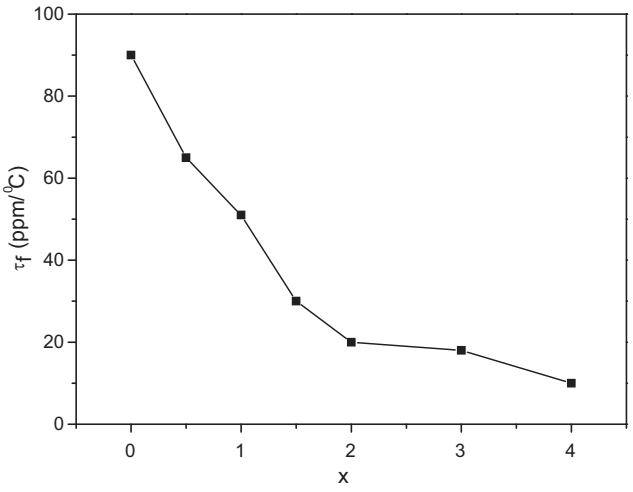

Fig. 5. The temperature coefficient of the resonant frequency (τ_f) of $Ba_3Ti_{4-x}(Zn_{1/3}Nb_{2/3})_xNb_4O_{21}$ $(0 \le x \le 4)$ ceramics sintered at 1250 °C for various values of x.

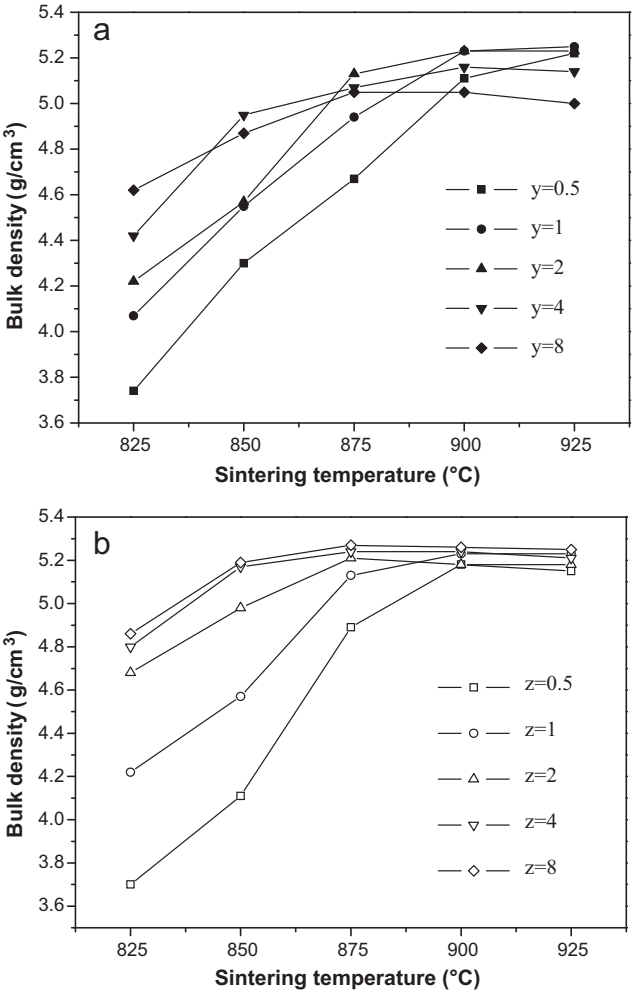

Fig. 6. Bulk densities of $Ba_3Ti_{4-x}(Zn_{1/3}Nb_{2/3})_xNb_4O_{21}$ $(x = 2)$ ceramics with (a) x wt% ZBS–1 wt% MC and (b) 2 wt% ZBS–y wt% MC as a function of sintering temperature.

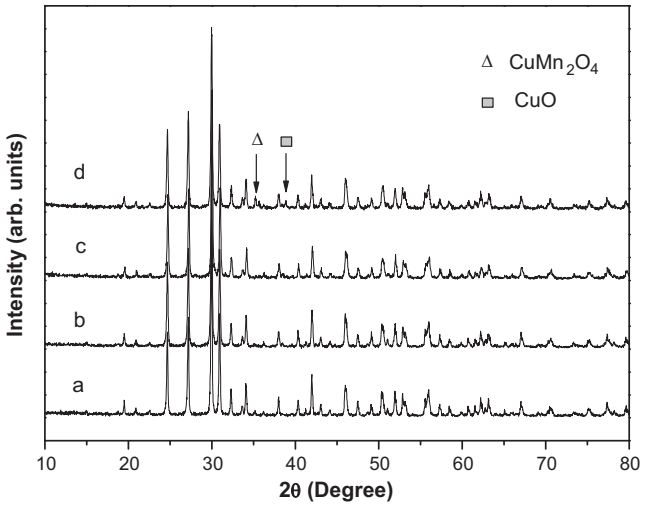

Fig. 7. X-ray diffraction patterns of $Ba_3Ti_{4-x}(Zn_{1/3}Nb_{2/3})_xNb_4O_{21}$ ($x=2$) ceramics with (a) 1 wt% MC–1 wt% ZBS, (b) 1 wt% MC–2 wt% ZBS, (c) 1 wt% MC–8 wt% ZBS and (d) 2 wt% ZBS–8 wt% MC.

of permittivity (τ_ε) as

$$\tau_f = -\left(\frac{1}{2}\tau_\varepsilon + \alpha_L\right), \tag{3}$$

where α_L is the linear thermal expansion coefficient.[20] τ_f is mainly dominated by the temperature coefficient of dielectric constant (τ_ε) owing to the negligible magnitude (~10 ppm/°C) of α_L. According to Bosman and Colla,[20,21] τ_ε (at constant pressure) is expressed as:

$$\tau_\varepsilon = \frac{1}{\varepsilon}\left(\frac{\partial\varepsilon}{\partial T}\right)_P = \frac{(\varepsilon-1)(\varepsilon-2)}{\varepsilon}(A+B+C), \tag{4}$$

$$A = \frac{1}{3\alpha_m}\left(\frac{\partial\alpha_m}{\partial T}\right)_V, \qquad B = \frac{1}{3\alpha_m}\left(\frac{\partial\alpha_m}{\partial V}\right)_T \times \left(\frac{\partial V}{\partial T}\right)_P,$$

$$C = \frac{1}{3V}\left(\frac{\partial V}{\partial T}\right)_P,$$

where α_m and V denote the polarizability and volume, respectively. The term A (commonly negative) represents the direct dependence of the polarizability on temperature. B and C represent the increase of the polarizability and the decrease of the number of polarizable ions in the unit-cell respectively; the unit cell volume increased with an increase in temperature. The B and C terms are normally the largest ones but have similar value with opposite signs, and the sum of B and C terms is approximately 6 ± 1 ppm/°C, therefore the term A plays a dominating role. The term A depends directly on the structures and their symmetries.

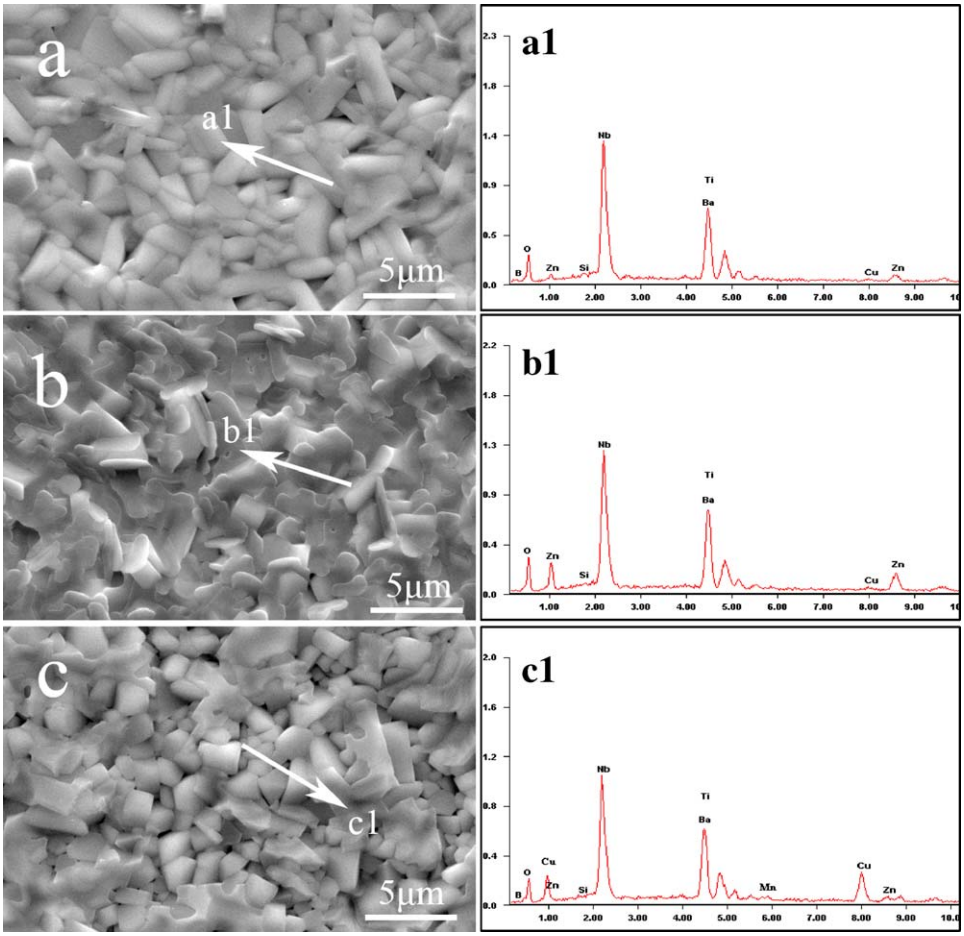

Fig. 8. SEM micrographs of $Ba_3Ti_{4-x}(Zn_{1/3}Nb_{2/3})_xNb_4O_{21}$ ($x=2$) ceramics with (a) 1 wt% MC–2 wt% ZBS, (b) 1 wt% MC–8 wt% ZBS, and (c) 2 wt% ZBS–8 wt% MC; (a1), (b1) and (c1) are the energy spectrum analysis of the corresponding spots in(a), (b) and (c), respectively.

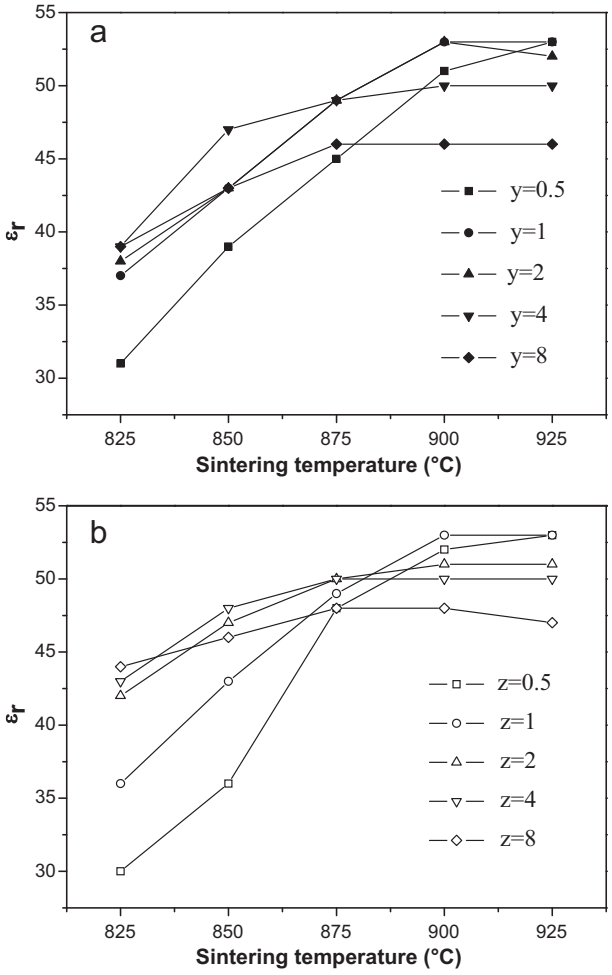

Fig. 9. Dielectric constants of $Ba_3Ti_{4-x}(Zn_{1/3}Nb_{2/3})_xNb_4O_{21}$ ($x=2$) ceramics with (a) y wt% ZBS–1 wt% MC and (b) 2 wt% ZBS–z wt% MC as a function of sintering temperature.

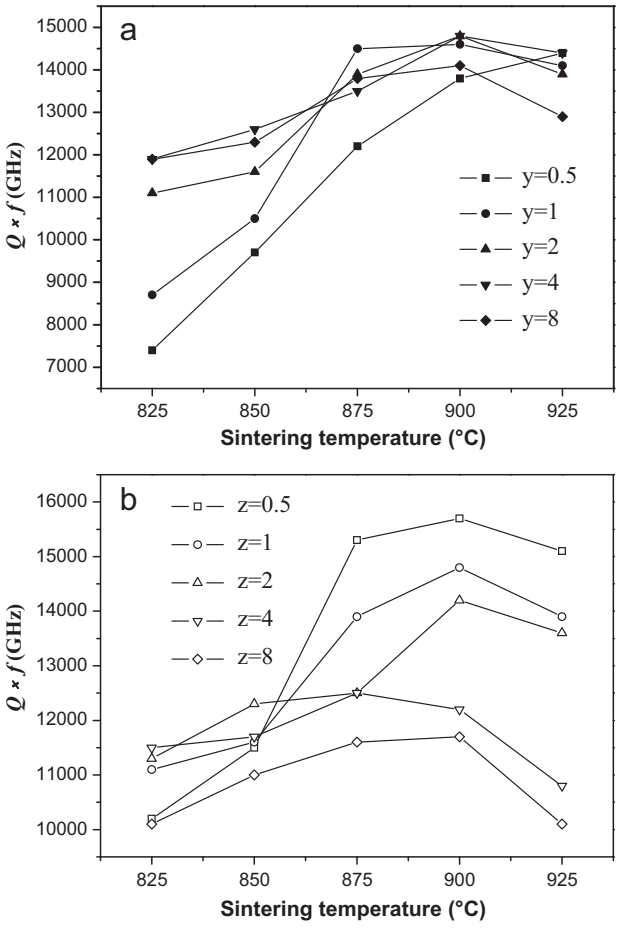

Fig. 10. $Q \times f$ values of $Ba_3Ti_{4-x}(Zn_{1/3}Nb_{2/3})_xNb_4O_{21}$ ($x=2$) ceramics with (a) y wt% ZBS–1 wt% MC and (b) 2 wt% ZBS–z wt% MC as a function of sintering temperature.

And the highly symmetric structure showed a direct polarizability temperature dependence bigger than for a tilted and distorted structure.[20] As the quantity of substitution of $(Zn_{1/3}Nb_{2/3})$ for Ti increasing, degree of tilting on oxygen octahedra was increased, and the structures of $Ba_3Ti_{4-x}(Zn_{1/3}Nb_{2/3})_xNb_4O_{21}$ ($0 \le x \le 4$) ceramics turned to be more distorted. Therefore, the τ_ε of $Ba_3Ti_{4-x}(Zn_{1/3}Nb_{2/3})_xNb_4O_{21}$ ($0 \le x \le 4$) ceramics decreased with increasing x value. As a result, τ_f decreased with increasing x.

Fig. 6 shows the bulk densities of $Ba_3Ti_{4-x}(Zn_{1/3}Nb_{2/3})_xNb_4O_{21}$ ($x=2$) ceramics with y wt% ZBS–1 wt% MC and 2 wt% ZBS–z wt% MC as a function of sintering temperature. In Fig. 6a, for the sample with $y=0.5$, the bulk densities increased gradually with increasing the sintering temperature, which indicated that the sintering temperature of this composition was higher than 925 °C. When $y>1$, the bulk densities of all samples reached the maximum values at 900 °C, and the bulk densities decreased with increasing the content of ZBS glass which was mainly due to the low density of ZBS. As shown in Fig. 6b, the densification temperature decreased from 925 to 875 °C with the z value increasing from 0.5 to 8. These results revealed that the additives of MC and ZBS can remarkably lower the sintering temperature of $Ba_3Ti_{4-x}(Zn_{1/3}Nb_{2/3})_xNb_4O_{21}$ ($x=2$) ceramics.

Fig. 7 shows the X-ray diffraction patterns of $Ba_3Ti_{4-x}(Zn_{1/3}Nb_{2/3})_xNb_4O_{21}$ ($x=2$) with various contents of MC and ZBS sintered at 900 °C for 2 h. It was evident

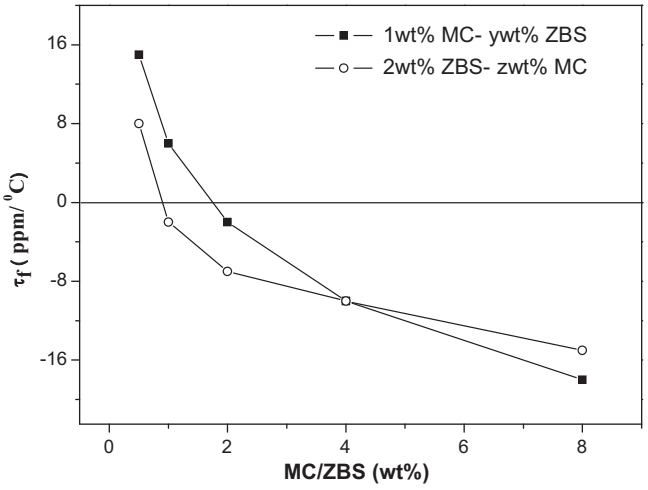

Fig. 11. The τ_f of $Ba_3Ti_{4-x}(Zn_{1/3}Nb_{2/3})_xNb_4O_{21}$ ($x=2$) ceramics as a function of MC or ZBS content sintered 900 °C for 2 h.

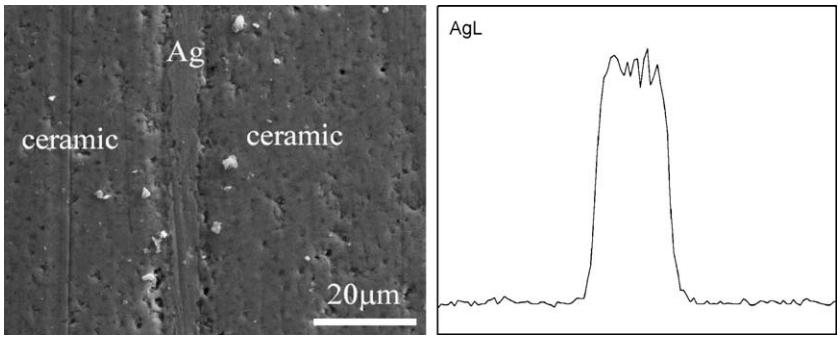

Fig. 12. EDS line scan of the interface between silver electrode and ceramic body.

that no second phase appeared with increasing ZBS glass content. However, CuO and $CuMn_2O_4$ phases which are the reaction product of $MnCO_3$ and CuO,[22] were detected for the sample with 2 wt% ZBS–8 wt% MC. SEM micrographs of $Ba_3Ti_{4-x}(Zn_{1/3}Nb_{2/3})_xNb_4O_{21}$ ($x=2$) with various contents of MC and ZBS sintered at 900 °C for 2 h are illustrated in Fig. 8. Specimen with 1 wt% MC–2 wt% ZBS showed a dense microstructure and elongated grains. However, as increasing the amount of MC or ZBS glass, it is clear that the morphologies of grain changed. Energy dispersive spectroscopy (EDS) analysis was used to reveal the effects of MC and ZBS glass on the microstructure of $Ba_3Ti_{4-x}(Zn_{1/3}Nb_{2/3})_xNb_4O_{21}$ ($x=2$). As shown in Fig. 8b1 and c1, Zn-rich and Cu-rich phases were identified in Fig. 8b and c, respectively. Zn-rich and Cu-rich phases, which were formed by ZBS or MC melting and then diffusing to $Ba_3Ti_{4-x}(Zn_{1/3}Nb_{2/3})_xNb_4O_{21}$ ($x=2$) ceramics during sintering, maybe affect the dielectric properties of $Ba_3Ti_{4-x}(Zn_{1/3}Nb_{2/3})_xNb_4O_{21}$ ($x=2$) ceramics.

Fig. 9 shows the dielectric constant of $Ba_3Ti_{4-x}(Zn_{1/3}Nb_{2/3})_xNb_4O_{21}$ ($x=2$) with various contents of MC and ZBS additives as a function of sintering temperature. The dielectric constant showed the similar tendency as the bulk densities. It is understood that a high density would lead to a high dielectric constant owing to lower porosity. More additions MC or ZBS glass caused the decrease of ε_r, which was probably attributed to the Zn-rich or Cu-rich secondary phase in Fig. 8.

Fig. 10 illustrates the $Q\times f$ values of $Ba_3Ti_{4-x}(Zn_{1/3}Nb_{2/3})_xNb_4O_{21}$ ($x=2$) ceramics with various contents of MC and ZBS additives as a function of sintering temperature. For almost all the specimens, with increasing the sintering temperature, the $Q\times f$ values increased and reached a maximum value and then decreased. The relationship between maximum $Q\times f$ value and ZBS content reveals the same trend between maximum density and ZBS content. The maximum $Q\times f$ value increased and then decreased slightly with the increase of ZBS content. The further addition of ZBS glass diminished the quality factor, which is due to lower density and more Zn-rich secondary phase. As shown in Fig. 10b, the saturated $Q\times f$ values decreased from 15,700 to 11,700 GHz with MC increasing from 0.5 to 8. It clearly indicated that MC was detrimental to the $Q\times f$ values, which was perhaps due to the generation of the Cu-rich secondary phase as shown in Fig. 8.

Fig. 11 shows the temperature coefficient of the resonant frequency of $Ba_3Ti_{4-x}(Zn_{1/3}Nb_{2/3})_xNb_4O_{21}$ ($x=2$) as a function of MC or ZBS content sintered at 900 °C for 2 h. The τ_f shifted toward the negative direction with increasing MC or ZBS content. It was evident that $Ba_3Ti_{4-x}(Zn_{1/3}Nb_{2/3})_xNb_4O_{21}$ ($x=2$) with a small amount of MC and ZBS could achieve a near zero τ_f.

For application as LTCC, Fig. 12 shows SEM micrographs and EDS line scan of the interface between the silver electrode and $Ba_3Ti_{4-x}(Zn_{1/3}Nb_{2/3})_xNb_4O_{21}$ ($x=2$) with 1 wt% MC–1 wt% ZBS tape co-fired at 900 °C for 2 h. The silver profile decreased sharply at the interface in Fig. 12, which indicated that the reaction between low fired $Ba_3Ti_{4-x}(Zn_{1/3}Nb_{2/3})_xNb_4O_{21}$ ($x=2$) ceramics and silver electrode did not occur. In order to evaluate the chemical compatibility of $Ba_3Ti_{4-x}(Zn_{1/3}Nb_{2/3})_xNb_4O_{21}$ ($x=2$) ceramic with silver, the mixtures of LTCC powder with 10 wt% Ag powders are heat-treated at 900 °C for 2 h. XRD of the mixtures is shown in Fig. 13. Since XRD patterns of the mixtures do not show the formation of secondary phase, it is considered that the LTCC material has a chemical compatibility with silver. Therefore, $Ba_3Ti_{4-x}(Zn_{1/3}Nb_{2/3})_xNb_4O_{21}$ ($x=2$) ceramics with 1 wt% MC–1 wt% ZBS combined additives could be selected as a promising candidate for LTCC application.

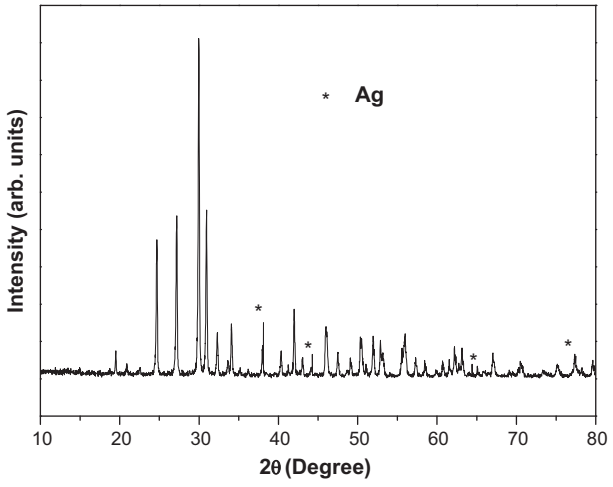

Fig. 13. X-ray diffraction patterns of LTCC sintered with 10 wt% Ag powder sintered at 900 °C for 2 h.

4. Conclusion

In this study, the effects of substitution of $(Zn_{1/3}Nb_{2/3})$ for Ti on the sintering behavior and microwave dielectric properties of $Ba_3Ti_{4-x}(Zn_{1/3}Nb_{2/3})_xNb_4O_{21}$ $(0 \le x \le 4)$ ceramics have been investigated. The dielectric constant (ε_r) and the temperature coefficient of the resonant frequency (τ_f) of $Ba_3Ti_{4-x}(Zn_{1/3}Nb_{2/3})_xNb_4O_{21}$ ceramics decreased with increasing x. However, the $Q \times f$ values increased with the substitution of $(Zn_{1/3}Nb_{2/3})$ for Ti. It was found that the proper additions of MC and ZBS glass to $Ba_3Ti_{4-x}(Zn_{1/3}Nb_{2/3})_xNb_4O_{21}$ $(x = 2)$ ceramics enabled a reduction in sintering temperature from 1250 to 900 °C. $Ba_3Ti_{4-x}(Zn_{1/3}Nb_{2/3})_xNb_4O_{21}$ $(x = 2)$ ceramics with 1 wt% MC and 1 wt% ZBS sintered at 900 °C for 2 h had a dense structure and showed good dielectric properties: $\varepsilon_r = 53$, $Q \times f = 14{,}600$ GHz, $\tau_f = 6$ ppm/°C. Also, this material was compatible with Ag electrodes, which made it as a promising material for LTCC application.

Acknowledgement

The authors thankfully acknowledge the financial support from National Key Technology Support Program (No. 2009BAG12A07).

References

1. Borisevich AY, Davies PK. Effect of V_2O_5 doping on the sintering and dielectric properties of M-phase $Li_{1+x-y}Nb_{1-x-3y}Ti_{x+4y}O_3$ ceramics. *J Am Ceram Soc* 2004;**87**:1047–52.
2. Tsunooka T, Androu M, Higashida Y, Sugiura H, Ohsato H. Effects of TiO_2 on sinterability and dielectric properties of high-Q forsterite ceramics. *J Eur Ceram Soc* 2003;**23**:2573–8.
3. Huang WT, Liu KS, Chu LW, Hsiue GH, Lin IN. Microwave dielectric properties of LTCC materials consisting of glass–$Ba_2Ti_9O_{20}$ composites. *J Eur Ceram Soc* 2003;**23**:2559–63.
4. Pamu D, Narayana Rao GL, James Raju KC. Effect of particle size and ZnO addition on microwave dielectric properties of nanocrystalline $(Zr_{0.8}Sn_{0.2})TiO_4$ ceramics. *Adv Appl Ceram* 2007;**106**:202–8.
5. Kang DH, Nam KC, Cha HJ. Effect of Li_2O–V_2O_5 on the low temperature sintering and microwave dielectric properties of $Li_{1.0}Nb_{0.6}Ti_{0.5}O_3$ ceramics. *J Eur Ceram Soc* 2006;**26**:2117–21.
6. Tong JX, Zhang QL, Yang H, Zou JL. Low-temperature firing and microwave dielectric properties of $Ca[(Li_{0.33}Nb_{0.67})_{0.9}Ti_{0.1}]O_{3-\delta}$ ceramics with LiF addition. *Mater Lett* 2005;**59**:3252–5.
7. Zheng H, Reaney IM, Muri D, Price T, Iddles DM. Effect of glass additions on the sintering and microwave properties of composite dielectric ceramics based on BaO–Ln_2O_3–TiO_2 (Ln = Nd, La). *J Eur Ceram Soc* 2007;**27**:4479–87.
8. Roberts GL, Cava RJ, Peck WF, Karjewski JJ. Dielectric properties of barium titanium niobates. *J Mater Res* 1997;**12**:526–30.
9. Ratheesh R, Sreemoolanadhan H, Suma S, Sebastain MT, Jose KA, Mohanan P. New high permittivity and low loss ceramics in the BaO–TiO_2–Nb_2O_5 composition. *J Mater Sci Mater Electron* 1998;**9**:291–4.
10. Sebastian MT. New low loss microwave dielectric ceramics in the BaO–TiO_2–Nb_2O_5/Ta_2O_5 system. *J Mater Sci Mater Electron* 1999;**10**:475–8.
11. Rajesh S, Babu SN, Potty SN, Ratheesh R. Preparation, characterization and dielectric properties of $Ba_{3-x}Sr_xM_4Ti_4O_{21}$ (M = Nb Ta and $0 \le x \le 3$) ceramics. *Mater Lett* 2006;**60**:2179–83.
12. Ko WJ, Choi YJ, Park JH, Park JG. Low-temperature sintering and microwave dielectric properties of $Ba_3Ti_{4-x}ZrxNb_4O_{21}$ ceramics with the substitution of Zr for Ti. *J Korean Phys Soc* 2006;**49**:1234–8.
13. Akbas MA, Davies AP. Cation ordering transformations in the $Ba(Zn_{1/3}Nb_{2/3})O_3$–$La(Zn_{1/3}Nb_{2/3})O_3$ system. *J Am Ceram Soc* 1998;**81**:1061–4.
14. Liu HX, Yu HT, Tian ZH, Meng ZH, Wu ZH, Ouyang SX. Dielectric properties of $(1-x)$ $CaTiO_3$–x $Ca(Zn_{1/3}Nb_{2/3})O_3$ ceramics system at microwave frequency. *J Am Ceram Soc* 2005;**88**:453–5.
15. Hakki BW, Coleman PD. A dielectric resonator method of measuring inductive in the millimeter range. *IEEE Trans Microwave Theory Tech* 1960;**16**:402–6.
16. Courtney WE. Analysis and evaluation of method of measuring the complex permittivity permeability of microwave insulators. *IEEE Trans Microwave Theory Tech* 1970;**18**:476–85.
17. Iddles DM, Bell AJ, Moulson AJ. *J Mater Sci* 1992;**27**:6303–7.
18. Shannon RD. Dielectric polarizabilities of ions in oxides and fluorides. *J Appl Phys* 1993;**73**:348–66.
19. Ogawa H, Taketani H, Kan A, Fujita A, Zouganelis G. Evaluation of electronic state of $Mg_4(Nb_{2-x}Sb_x)O_9$ microwave dielectric ceramics by first principle calculation method. *J Eur Ceram Soc* 2005;**25**:2589–863.
20. Bosman AJ, Havinga EE. Temperature dependence of dielectric constants of cubic ionic compounds. *Phys Rev* 1963;**129**:1593–600.
21. Colla EL, Reaney IM, Setter N. Effect of structural changes in complex perovskites on the temperature coefficient of the relative permittivity. *J Appl Phys* 1993;**74**:3414–25.
22. Zou D, Zhang QL, Yang H, Ma MC. Low-temperature sintering and microwave dielectric properties of $Ba_3Ti_4Nb_4O_{21}$ with $MnCO_3$–CuO. *J Mater Sci Mater Electron* 2008;**19**:1000–4.